The Multifaceted Nature of Gallides

Michael Baitinger[##], Lev Akselrud, Bodo Böhme, Ulrich Burkhardt, Xian-Juan Feng, Primož Koželj, Mitja Krnel, Alim Ormeci, Yurii Prots, Marcus Schmidt, Igor Veremchuk, Frank R. Wagner, Chia-Chi Yu and Yuri Grin[#]

Gallium exhibits a remarkable diversity of crystal structures in both intermetallic compounds and its elemental form. Intermetallic gallides exist at the boundary between 2c-2e bonding in Zintl polyanions, multicenter bonding in Wade clusters and metal structures. Our recent study of the Na/Ga system, which had been considered resolved for decades, has provided new insights into the crystal chemistry of gallides and yielded surprising results. The study exemplifies the strategies established throughout the department's history.

Metastable intermetallic phases or those with low thermal stability cannot be obtained by traditional high-temperature methods. Instead, alternative preparation routes were developed, where precursors are oxidized at moderate temperatures in ionic liquids or an oxidizing gas atmosphere [1 – 4]. This method also provides access to the low-temperature region of phase diagrams and allows the detection of unknown phases, as demonstrated in this report for the Na-Ga system. So far, three phases – $NaGa_4$, Na_7Ga_{13}, and $Na_{22}Ga_{39}$ – have been reported, each with distinct structural organization. We began our study by reacting the highly sensitive Na_7Ga_{13} phase with gaseous NH_3 to find further metastable compounds [5]. After a series of experiments with varying reaction times, the mechanism of the redox reaction at 300 °C was elucidated (Figure 1). Initially, Na_7Ga_{13} is oxidized by NH_3 to form $NaGa_4$, $NaNH_2$, and H_2(g). Subsequently, $NaNH_2$ decomposes into elemental Na, which reduces $NaGa_4$ to Na_2Ga_7. Concurrently, Na_2Ga_7 is formed by the comproportionation of $NaGa_4$ with the remaining Na_7Ga_{13}. Finally, and with longer reaction times, Na_2Ga_7 reacts with excess NH_3 to $NaGa_4$. Higher reaction temperatures led to the formation of GaN.

Based on the reaction mechanism (Figure 1), Na_2Ga_7 is a thermodynamically stable equilibrium phase, not a metastable one. This finding contradicted the previously well-established phase diagram. However, annealing the elemental components for 7 days at temperatures ranging from 200 °C to 450 °C yielded single-phase Na_2Ga_7. The lattice parameters of Na_2Ga_7 did not change in the two-phase regions $NaGa_4$/Na_2Ga_7 and Na_2Ga_7/Na_7Ga_{13}, while DTA experiments clearly revealed an endothermic decomposition at T = 501 °C. Therefore, Na_2Ga_7 is an equilibrium phase with a constant composition. The crystal structure of Na_2Ga_7 (Z = 8) closely resembles that of the borosilicides $MgB_{12}Si_2$ [6] and $Li_2B_{12}Si_2$ [7] (Z = 4). These compounds share a topologically similar arrangement of interconnected icosahedral clusters and four-bonded atoms (Figure 2 and 3). The $[(12b)B_{12}]^{2-}$ Wade clusters in the borosilicides correspond to $[(12b)Ga_{12}]^{2-}$ icosahedra in Na_2Ga_7 and the $[(4b)Si]^0$ to the $[(4b)Ga]^-$ units. The anionic framework consists of strongly puckered hexagon layers perpendicular to [001], incorporating icosahedral clusters. Within each layer, each three adjacent hexagons form troughs that can accommodate cations. In $Li_2B_{12}Si_2$ (space group *Cmce*), these troughs are completely filled with Li atoms (Figure 2a). $MgB_{12}Si_2$, with only half the cations, exhibits partially filled troughs and reduced symmetry (space group *Pnma*; Figure 2b). Na_2Ga_7, having twice as many cations as $Li_2B_{12}Si_2$, exhibits *Pnma* symmetry with an additional Na position (Figure 2c). In summary, Na_2Ga_7 represents a filled variant of the $Li_2B_{12}Si_2$ type structure, where the increased cation content results in a more complex structural organization. Na_2Ga_7 is an electronically balanced Zintl-Wade phase with the formula $[Na^+]_4[(Ga_{12})^{2-}]\,[Ga^-]_2$. It is diamagnetic and, based on electronic structure calculations, a semiconductor with a band gap of 0.29 eV. Once the thermodynamic stability of Na_2Ga_7 was demonstrated, it made sense to undertake substitution experiments to explore the variability of the structure type for different chemical compositions. At first, the substitution of Na with Li was examined [8].

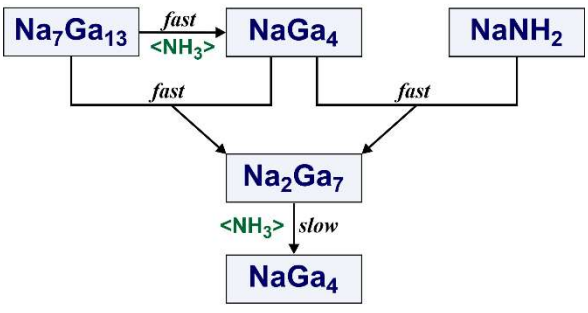

Fig. 1: Reaction products during treatment of Na_7Ga_{13} with gaseous NH_3 at 300 °C.

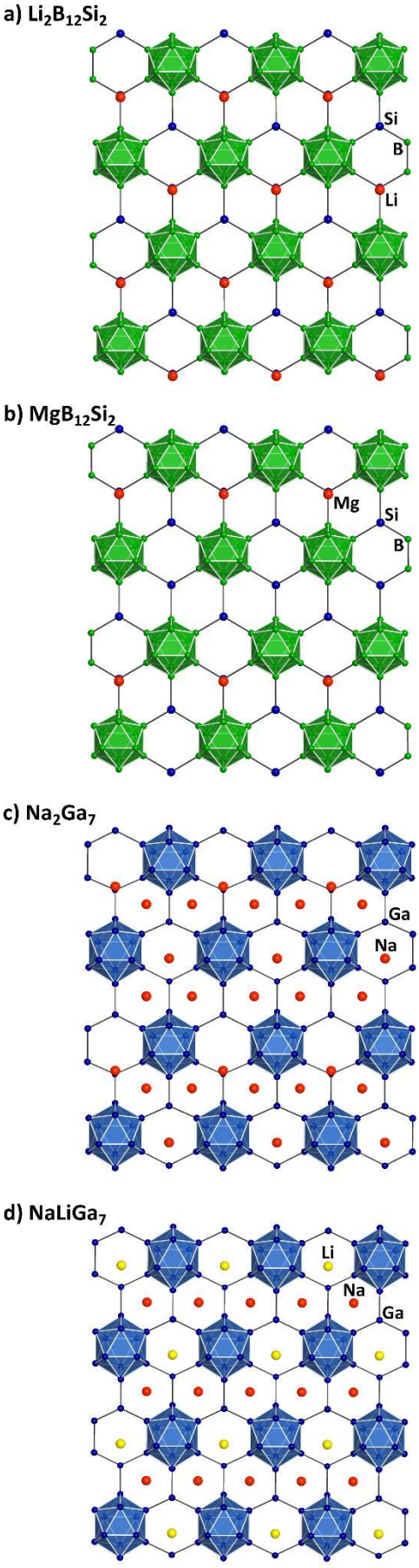

Fig. 2: Representatives of the $MgB_{12}Si_2$ family.

Single-phase samples of composition $Na_{2-x}Li_xGa_7$ ($x \leq 1$) were synthesized from the elements at 300 °C or by the ion exchange reaction of Na_2Ga_7 with LiCl. The boundary compositions Na_2Ga_7 and $Na_1Li_1Ga_7$ crystallize with different structure types related by a group-subgroup dependence. Na-rich compositions ($x \leq 0.5$) represent a substitutional solid solution (space group *Pnma*), the Li-rich compositions feature an unconventional replacement mechanism in which Li atoms occupying interstitial positions induce vacancies at the Na positions (space group *Cmce*). The arrangement of cations makes $NaLiGa_7$ another new structure type within the $MgB_{12}Si_2$ structure family (Figure 2d). As for Na_2Ga_7, band structure calculations and diamagnetic susceptibility measurements for $NaLiGa_7$ indicate semiconducting behavior. The formation temperatures in the series $Na_{2-x}Li_xGa_7$ decrease with increasing Li content from 501(2) °C ($x = 0$) to 489(2) °C ($x = 1$).

With respect to the anionic Ga network, an investigation was conducted to determine the extent to which Ga atoms can be isoelectronically substituted by In and whether cation ordering can be achieved by expanding the host framework [9]. A ternary solid solution $Na_2Ga_{7-x}In_x$ ($x \leq 0.25$) was synthesized by annealing the elements at 300 °C in sealed Ta ampoules. The decomposition temperature decreased with increasing In content from 501(2) °C ($x = 0$) to 474(2) °C ($x = 0.25$). Although the solubility of In turned out to be small, even a minor In content significantly affects the crystal structure, leading to a noticeable expansion of the unit cell volume. The position of the In atoms within the Ga framework was determined by crystal structure analysis. The In atoms were found to substitute solely one of the two four-bonded Ga framework positions (Figure 3). This behavior can be rationalized by considering steric demands.

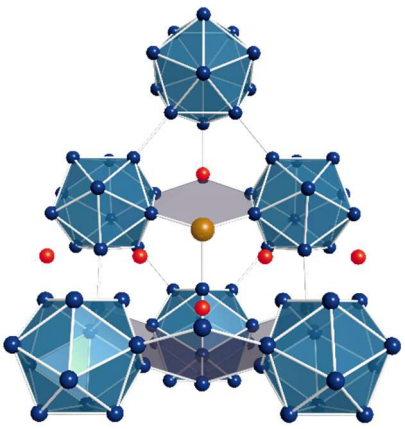

Fig. 3: Position of the In atoms in the framework of $Na_2Ga_{7-x}In_x$ (In atom orange, Na – red, Ga – blue).

With the discovery of a new phase, thermoanalytical investigations became necessary to update the Na/Ga phase diagram [10]. The decomposition of Na_2Ga_7 was determined through DSC experiments at 501°C, where the phase decomposes peritectically to Na_7Ga_{13} and melt (Figure 4a). This temperature is only slightly above the decomposition of $NaGa_4$ at 495°C. As a result, the portion of Na_2Ga_7 at the liquidus curve is very small, and the phase does not form in detectable amounts from the melt. This is why Na_2Ga_7 was overlooked for such a long time, and the binary system was never examined more closely at this point. Na_7Ga_{13} melts peritectically at 545°C, which is only slightly lower than the congruent melting of $Na_{22}Ga_{39}$ at 549°C (Figure 4b). Due to the small difference in compositions, previous reports considered only one of the two phases, either Na_7Ga_{13} or $Na_{22}Ga_{39}$, as the equilibrium phase in the phase diagram. In the Na-rich region, the critical point of the liquid two-phase system was found at T_c = 523°C, which had previously been predicted to be 740°C. The monotectic temperature of $Na_{22}Ga_{39}$ and liquid Na was determined to be 495°C. Elemental Na and $Na_{22}Ga_{39}$ do not form a eutectic. A solid solution of Ga in Na decomposes peritectically, but less than 0.2°C above the melting point of elemental Na.

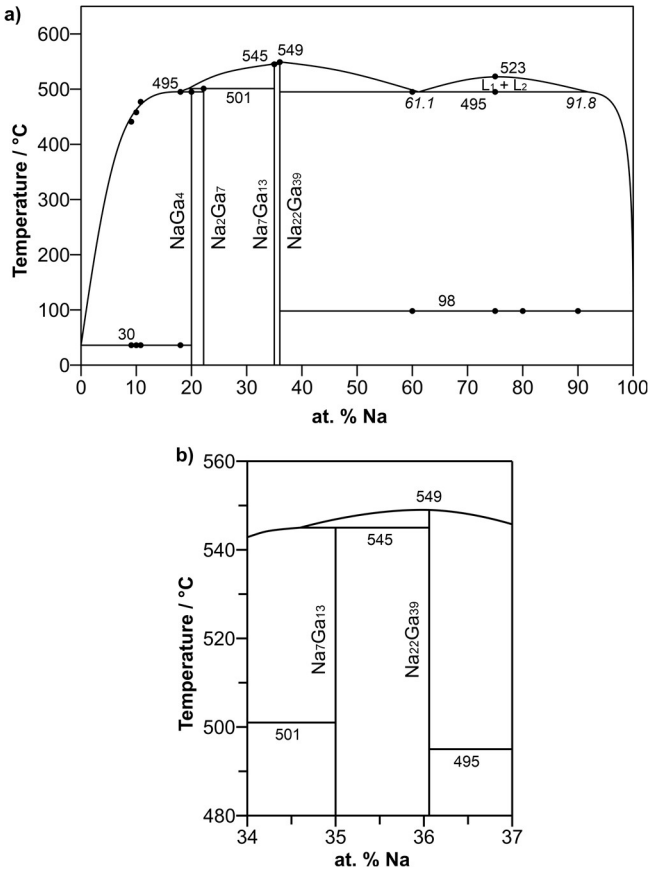

Fig. 4: Revised phase diagram of the Na-Ga system.

To accurately determine the minor differences in thermal effects, samples were also measured relative to each other (*MR-DTA* method [10]). The corrections to the Na/Ga phase diagram are significant. The study of phase formation remains indispensable for rational synthesis planning and crystal growth.

While investigating the composition ranges in the Na-Ga system, we noticed peculiar features in the crystal structure of $NaGa_4$ that prompted a reexamination [11]. The *c*/*a* ratio for $NaGa_4$ is much larger than in the other MGa_4 gallides, and the *c* lattice parameter even surpasses that of $BaGa_4$ by far. The $BaAl_4$ type of structure of $NaGa_4$ is fundamental in solid-state science and is characterized by condensed 18-atom cages that accommodate electropositive metal atoms (Figure 5). The chemical bonding of the $BaAl_4$ type can conceptually be understood as infinite 2D layers of edge-condensed *nido* Al_5 Wade clusters. Adjacent layers are connected via 2-center-2-electron bonds along [001] (see [11]).

In Ba_2Ga_8 (= $BaAl_4$ with Z = 2), a total of 28 electrons (2 × 2 + 8 × 3) is available per unit cell. Applying the count for the *nido* Wade Ga_5 cluster, 24 electrons (4 × 6) are required for the formation of the four clusters per unit cell, leaving 4 electrons for the two 2c-2e bonds. In Na_2Ga_8 (= $NaAl_4$ with Z = 2), only 26 electrons are available per unit cell, indicating a relative deficiency of bonding electrons. Consequently, one might expect the interatomic distances in the framework of $NaGa_4$ to increase. However, contrary to expectations, the distances *d*(Ga–Ga) are similar to those in the $EuGa_4$ and significantly shorter than in $SrGa_4$ and $BaGa_4$. Therefore, the enlarged *c*-parameter is caused by steric factors rather than the valence electron effect. In the series MGa_4, (*M* = Ba, Sr, Eu), volume changes are mainly

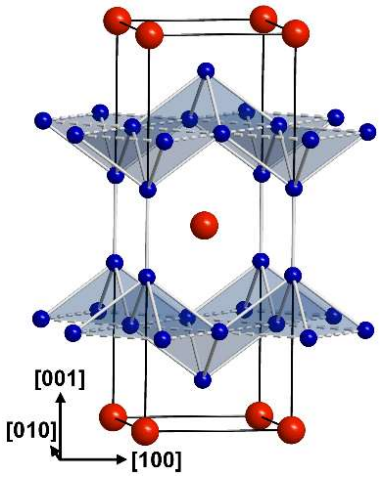

Fig. 5: Unit cell of $NaGa_4$ with focus on the condensed nido Wade clusters (Na atoms – red, Ga atoms – blue).

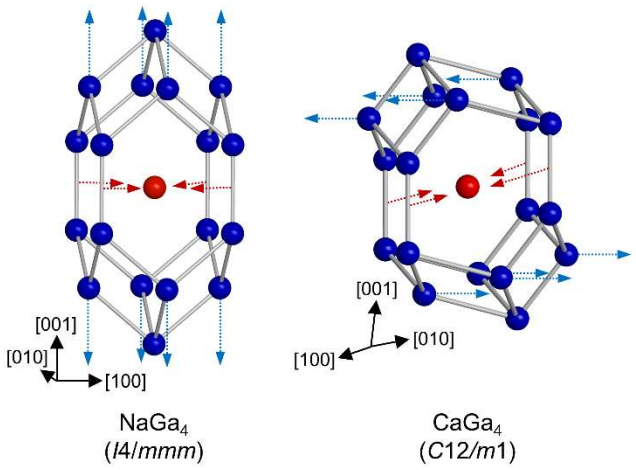

Fig. 6: Subtypes of the $BaAl_4$ type of structure allowing the adaption to small cations.

achieved through continuous changes in bond distances. However, for $EuGa_4$, the shortest interatomic distance in the Ga framework reaches the value of the shortest bond in α-Ga. When the distances can no longer be compressed, volume adaptation to the smaller Na atoms is achieved by changing the bond angles. Consequently, the *c*-axis in $NaGa_4$ is significantly enlarged (Figure 6). The adaption of the $NaGa_4$ structure thus constitutes a sub-type of the $BaAl_4$ type for particularly small cations, resulting in the largest *c*/*a* ratio among all MGa_4 compounds. Another known subtype of $BaAl_4$ is the $CaGa_4$ type with a monoclinic distortion variant (Figure 6).

Detailed single crystal structure analysis of $NaGa_4$ after heat treatment at 300°C led to the identification of a 2D defect, observed for the first time in the $BaAl_4$ type of structure. A small fraction of Na atoms and Ga_2 dumbbells exchange their positions (Figure 7). Structural distortion is minimized if the defect positions are arranged in common (001) planes. By introducing defect positions, the Ga–Ga distances do not change. However, the tetrahedral coordination in the regular structure motif transforms into a square-planar arrangement, which may serve as an interface to the elemental Ga structure and potentially explain a solid solution of Na in elemental Ga.

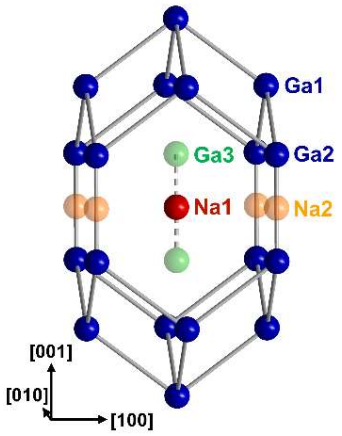

Fig. 7: Defect in the $NaGa_4$ structure observed in single crystals annealed at 300°C.

ELI-D analysis reveals a clear distinction between fully occupied inter-cluster and fractionally occupied skeletal bonds. In fact, three atoms (Ga2 + Ga2 + Na1) contribute to the Ga2–Ga2 bond basin (Figure 7) with 0.55 electrons (0.27 + 0.27 + 0.01, respectively), while four atoms (Ga1 + Ga2 + Na1 + Na1) contribute to the Ga1–Ga2 bond basin with 1.46 electrons (0.77 + 0.54 + 0.01 + 0.01, respectively). Hence, Na atoms make a minor contribution to the Ga–Ga bonds (Figure 8). The Bader charges display the different characteristics of the Ga species: Na (+0.78), Ga1 (–0.08), and Ga2 (–0.30).

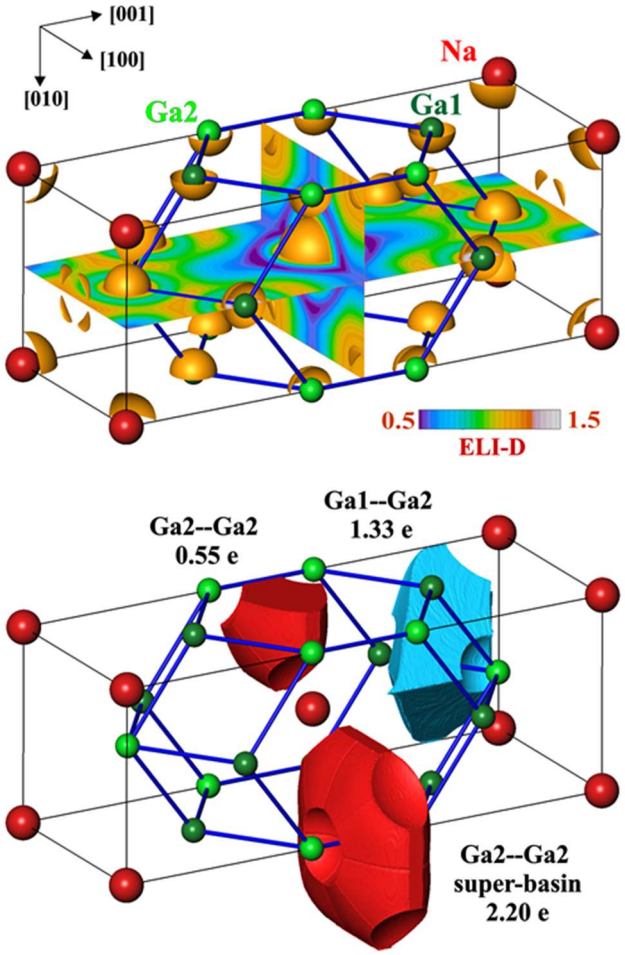

Fig. 8: ELI-D distribution in $NaGa_4$. Top: ELI-D isosurfaces and ELI-D maps in (200) and (002) planes; bottom: the Ga2-Ga2 (red) and Ga1-Ga2 (blue) bond basins.

References

[1] *A guest-free germanium clathrate, A. M. Guloy, R. Ramlau, Z. Tang, W. Schnelle, M. Baitinger, Y. Grin, Nature* ***443*** *(2006) 320–323,* https://doi.org/10.1038/nature05145

[2] *Oxidation of M_4Si_4 (M = Na, K) to Clathrates by HCl or H_2O, B. Böhme, A. Guloy, Z. Tang, W. Schnelle, U. Burkhardt, M. Baitinger, Y. Grin, JACS* ***129*** *(2007) 5348–5349,* https://doi.org/10.1021/ja0705691

[3] *Synthesis of the Clathrate-I Phase $Ba_{8-x}Si_{46}$ via Redox Reactions, Y. Liang, B. Böhme, M. Reibold, W. Schnelle, U. Schwarz, M. Baitinger, H. Lichte, Y. Grin, Inorg. Chem.* ***50*** *(2011) 4523–4528,* https://doi.org/10.1021/ic2001859

[4]* *Type-II Clathrate $Na_{24-\delta}Ge_{136}$ from a Redox-Preparation Route, X.-J. Feng, M. Bobnar, S. Lerch, H. Biller, M. Schmidt, M. Baitinger, T. Strassner, Y. Grin, B. Böhme, Chem. Eur. J.* ***27*** *(2021) 12776–12787,* https://doi.org/10.1002/chem.202102082

[5]* *Na_2Ga_7: A Zintl–Wade Phase Related to "α-Tetragonal Boron, C.-C. Yu, A. Ormeci, I. Veremchuk, X.-J. Feng, Yu. Prots, M. Krnel, P. Koželj, M. Schmidt, U. Burkhardt, B. Böhme, L. Akselrud, M. Baitinger, Y. Grin, Inorg. Chem.* ***62*** *(2023) 9054–9062,* https://doi.org/10.1021/acs.inorgchem.3c00790

[6] *Synthesis and crystal structure of $MgB_{12}Si_2$ – The first ternary compound in the system B/Mg/Si, T. Ludwig, H. Hillebrecht, J. Solid State Chem.* ***79*** *(2006) 1623–1629,* https://doi.org/10.1016/j.jssc.2006.02.013

[7] *$Li_2B_{12}Si_2$: The First Ternary Compound in the System Li/B/Si: Synthesis, Crystal Structure, Hardness, Spectroscopic Investigations, and Electronic Structure, N. Vojteer, M. Schroeder, C. Röhr, H. Hillebrecht, Chem. Eur. J.* ***14*** *(2008) 7331–7342,* https://doi.org/10.1002/chem.200701949

[8]* *Ordering by cation replacement in the system $Na_{2-x}Li_xGa_7$, C.-C. Yu, Yu. Prots, A. Ormeci, M. Krnel, M. Schmidt, L. Akselrud, F. R. Wagner, Y. Grin, M. Baitinger, Dalton Trans.* ***53*** *(2023) 908–916,* https://doi.org/10.1039/D3DT03628F

[9]* *The Solubility of Indium in Na_2Ga_7, C.-C. Yu, Yu. Prots, Y. Grin, M. Baitinger, Eur. J. Inorg. Chem.* ***27*** *(2024), e202400016,* https://doi.org/10.1002/ejic.202400016

[10] *The Na/Ga phase diagram, in preparation for Acta Mat.*

[11]* *Adaptation of the $BaAl_4$ type to small cations: the case of $NaGa_4$, C.-C. Yu, Yu. Prots, P. Koželj, F. R. Wagner, M. Baitinger, Y. Grin, Chem. Eur. J. (2024), e202402457,* https://doi.org/10.1002/chem.202402457

[##] michael.baitinger@cpfs.mpg.de

[#] grin@cpfs.mpg.de